

Statics and Dynamics of Vortex Liquid Crystals

C. Reichhardt and C.J. Olson Reichhardt

Theoretical Division and Center for Nonlinear Studies, Los Alamos National Laboratory, Los Alamos, New Mexico 87545
(November 20, 2018)

Using numerical simulations we examine the static and dynamic properties of the recently proposed vortex liquid crystal state. We confirm the existence of a smectic-A phase in the absence of pinning. Quenched disorder can induce a smectic state even at $T = 0$. When an external drive is applied, a variety of anisotropic dynamical flow states with distinct voltage signatures occur, including elastic depinning in the hard direction and plastic depinning in the easy direction. We discuss the implications of the anisotropic transport for other systems which exhibit depinning phenomena, such as stripes and electron liquid crystals.

PACS numbers: 74.25.Qt

Recently, a new state of vortex matter termed a vortex liquid crystal was proposed to occur in superconductors with anisotropic vortex-vortex interactions [1]. In such systems, the vortex lattice first melts in the soft direction, giving rise to an intermediate vortex smectic-A state, followed at higher temperatures by a melting into a nematic state. The initial theoretical calculations of this transition combined an elastic model with the Lindemann criterion for melting; however, the validity of this approach has been called into question [2,3]. The Lindemann criterion does not take into account the proliferation of dislocations that is likely to occur in a smectic-A state, so a numerical investigation would be very useful both to determine whether the smectic-A state can occur in the vortex system as well as to examine the dynamics of vortex liquid crystals in the presence of disorder. The physics of the vortex liquid crystal state should be generic to the class of problems which can effectively be modeled as a two-dimensional (2D) system of particles with anisotropic repulsive interactions. Such a system has already been physically realized for magnetic colloidal particles, where a smectic-A state was observed along with dislocations that have preferentially aligned Burgers vectors [4]. There is also considerable interest in electron liquid crystal states, which may arise when anisotropic interactions in classical electron crystals give rise to smectic and nematic states [5,6]. Evidence for such states has been observed in transport measurements which show hard and soft directions for flow [7,8].

Previous studies of vortex smectic states considered vortices interacting with some form of an underlying 1D periodically modulated substrate [9]. A very similar system in which smectic states have been observed is colloidal particles interacting with 1D periodic substrates [10]. Each of these systems melts into an intermediate smectic-C state. When the underlying substrate is disordered rather than periodic, application of an external drive induces an anisotropic fluctuating force that organizes the vortices into a moving smectic state, where the dislocations in the vortex lattice are aligned with the direction of the applied drive [11,12]. In the case of the proposed vortex liquid crystal state, the anisotropy arises

when the vortex cross section becomes elliptical due to an anisotropic superfluid stiffness which leads to different effective masses in the three crystalline directions [1]. The theoretical calculations in Ref. [1] were performed for a system with no quenched disorder; however, real superconductors often contain significant amounts of random pinning. It would be desirable to understand the transport properties of vortex liquid crystals in order to identify signatures of the liquid crystal phase and seek new types of dynamical phenomena in these systems. Understanding how quenched disorder affects an anisotropic system of repulsively interacting particles is also relevant to dynamics in electron liquid crystal states.

To address these issues, we consider a 2D system of N_v interacting vortices with periodic boundary conditions in the x and y directions. The overdamped equation of motion for a single vortex i is

$$\eta \frac{d\mathbf{R}_i}{dt} = \mathbf{f}_i^{vv} + \mathbf{f}_i^T + \mathbf{f}_i^p + \mathbf{f}_i^d \quad (1)$$

The damping constant η is set to unity. The vortex-vortex interaction force is $\mathbf{f}_i^{vv} = \sum_{j \neq i}^{N_v} A_v K_1(r_{ij}/\lambda) \hat{\mathbf{r}}_{ij}$, where K_1 is the modified Bessel function, which decays exponentially for large distances, λ is the London penetration depth, A_v is the vortex interaction prefactor, and r_{ij} is the distance between vortices i and j . The Bessel function is appropriate for stiff, 3D vortex lines. We have also considered $1/r$ interaction potentials appropriate for thin film superconductors as well as Yukawa interaction potentials for colloidal particles and find the same qualitative features. The thermal force \mathbf{f}_i^T arises from random Langevin kicks with the properties $\langle \mathbf{f}_i^T \rangle = 0$ and $\langle \mathbf{f}_i^T(t) \mathbf{f}_j^T(t') \rangle = 2\eta k_B T \delta(t - t') \delta_{ij}$. The quenched disorder \mathbf{f}_i^p is modeled as random pinning sites in the form of attractive parabolic traps of radius $r_p = 0.2\lambda$ and strength f_p . The Lorentz driving force from an external applied current is \mathbf{f}^d . The system size is measured in units of λ and the forces in terms of A_v . The anisotropic interactions are introduced by multiplying the vortex-vortex interaction force in the x and y directions by a vector (C_x, C_y) , where the anisotropy $C = C_x/C_y$. In this work we concentrate on the case $C = 1/\sqrt{10}$ which

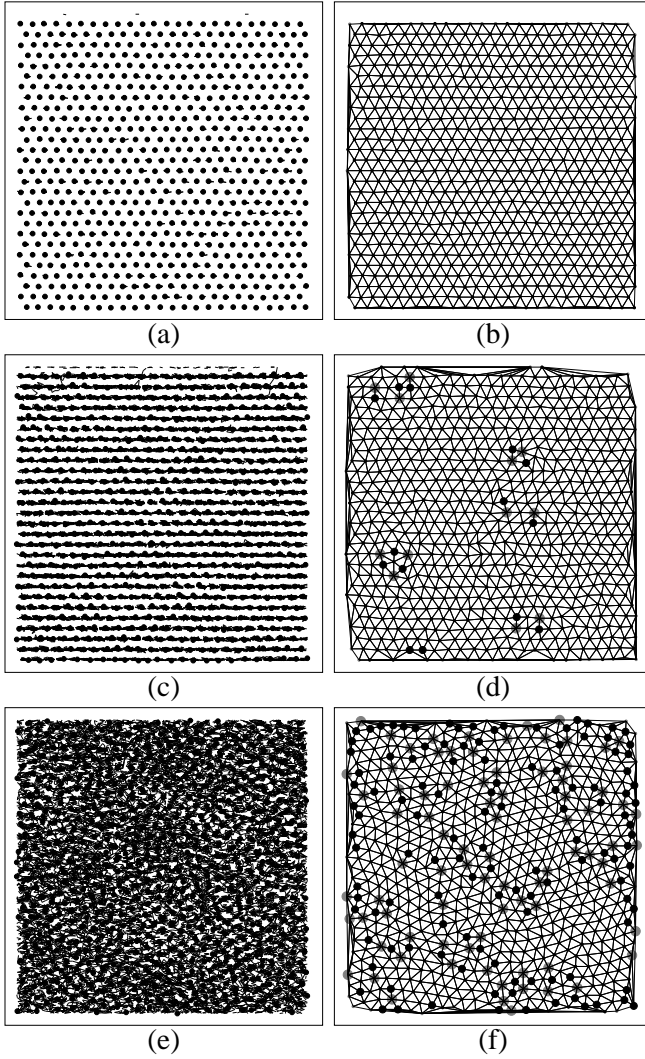


FIG. 1. (a,c,e) Black dots: vortices; black lines: vortex trajectories. (b,d,f) Delaunay triangulation, with topological defects (5 and 7-fold coordinated particles) marked as filled circles. (a,b) $T = 0.5$; (c,d) $T = 1.2$; (e,f) $T = 1.35$.

is the value considered in Ref. [1]. We take the x axis to be the soft direction and the y axis as the hard direction.

We first consider the case where the pinning and the external driving force are absent. In Fig. 1 we illustrate the melting of a $24\lambda \times 24\lambda$ system with a vortex density of $\rho_v = 1.2/\lambda^2$. Figure 1(a) shows the vortex positions (dots) and trajectories (lines) for a fixed period of time with a fixed $T = 0.5$, and Fig. 1(b) shows a corresponding Delaunay triangulation. At this temperature, the system remains in a crystalline state with no dislocations. The vortices are undergoing larger random displacements in the soft (x) direction than in the hard (y) direction; however, there is no long time diffusion of the particles. Figures 1(c) and 1(d) present the smectic-A state at $T = 1.2$. Here the trajectories have a 1D liquid structure with

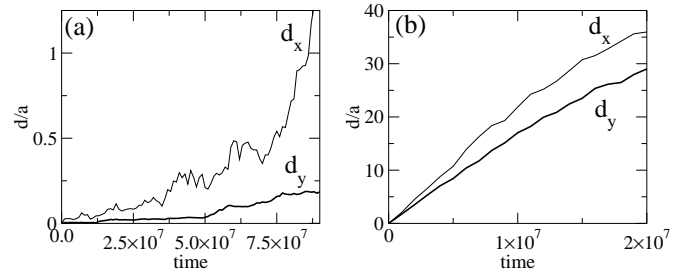


FIG. 2. The average particle displacements in each direction, d_x and d_y , normalized by the lattice constant a , vs time, measured in molecular dynamics steps. (a) The smectic-A state at $T = 1.21$. (b) The nematic phase at $T = 1.35$.

motion along the soft x direction and no significant translation of the vortices in the y direction. The Delaunay triangulation indicates the presence of dislocations with aligned Burgers vectors, which is characteristic of the smectic-A state. Figures 1(e) and 1(f) illustrate the vortex liquid phase at $T = 1.35$. The vortex trajectories show clear diffusion in both the x and y directions, with more pronounced motion in the x direction. The dislocations are no longer aligned in a single direction, indicating the loss of long-range order in both the x and y directions. These results confirm that a smectic-A state can occur in a system of vortices with anisotropic interactions, as predicted by theoretical calculations [1]. We note that when the anisotropy ratio C is too small, the two-step melting transition illustrated here is lost.

To further characterize the smectic state, in Fig. 2 we plot the average particle displacements for the x and y directions, $d_x = \langle \sum_i^{N_v} |x_i(t) - x_i(t')| \rangle / N_v$ and $d_y = \langle \sum_i^{N_v} |y_i(t) - y_i(t')| \rangle / N_v$. In the smectic phase at $T = 1.21$, shown in Fig. 2(a), d_x/a increases much more rapidly than d_y/a , and does not saturate but increases to a value over 1, indicating that the vortices can diffuse more than a lattice constant in the x direction over time. This is due to the formation of dislocations which allow adjacent rows of vortices to slip past each other while remaining confined in the y direction. We note that the saturation value of d_y/a is approximately $1/5$, larger than the Lindemann criterion value of $1/10$. Excess motion in the y direction occurs during a sliding event when two rows slip past each other and the vortices in each row are temporarily displaced in the direction perpendicular to the slip plane. This transverse motion is not large enough to permit the formation of dislocations aligned in the hard direction. In the nematic phase, shown in Fig. 2(b) at $T = 1.35$, d_x still increases more rapidly than d_y ; however, the continuous increase of both quantities indicates that the particles are diffusing throughout the entire system.

We next consider the effect of random disorder by adding $N_p = 2N_v$ randomly located pinning sites to the same system studied in Fig. 1, and then conducting a

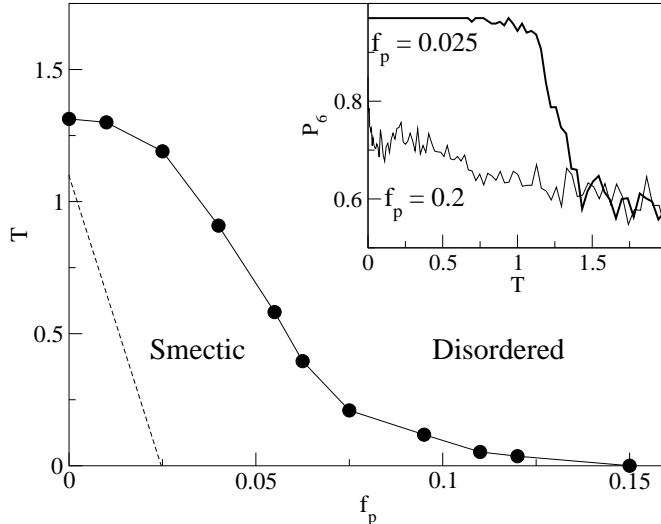


FIG. 3. Regions in which the smectic and disordered phases occur in a system with quenched disorder as a function of temperature T and pinning strength f_p . Dashed line roughly indicates the weak pinning region in which a 2D anisotropic Bragg glass forms. Inset: the density of six-fold coordinated particles P_6 vs T for (top curve) $f_p = 0.025$ and (bottom curve) $f_p = 0.2$.

series of simulations at varied T and varied pinning strength f_p . For high temperatures we always obtain a nematic phase, while at $T = 0$ for large f_p we find a pinned nematic phase. At low T and low f_p we observe a phase very similar to that shown in Fig. 1(c,d), where the vortex lattice is oriented in the soft direction and there are a small number of aligned dislocations. We term this a pinned smectic-A phase. In Fig. 3 we indicate the regions in which the smectic and disordered phases appear as a function of temperature and pinning strength. The phase boundary is identified via the density of sixfold coordinated particles, P_6 ; the defect density is given by $1 - P_6$. In the crystal phase, there are no defects and $P_6 = 1$. In the smectic phase, $P_6 = 0.91$ to 0.95 , and in the nematic phase $P_6 > 0.8$. In the inset of Fig. 3 we plot P_6 vs T for two different disorder strengths. For $f_p = 0.025$ (upper line) the system is in the pinned smectic state at $T = 0$. As T increases, there is a clear transition to the disordered state, as indicated by the drop in P_6 near $T = 1.19$. The lower line shows P_6 for $f_p = 0.2$, when the pinning is strong enough to disorder the system even at $T = 0$. These results suggest that weak random disorder can increase the extent of the regions where the smectic-A phase occurs when there are anisotropic interactions, by suppressing the crystalline phase at low temperatures and raising the melting temperature of the smectic state.

It has been shown that dislocations are always present for weak disorder in two dimensional isotropic systems; however, the distance between the dislocations can be arbitrarily large compared to the range of the

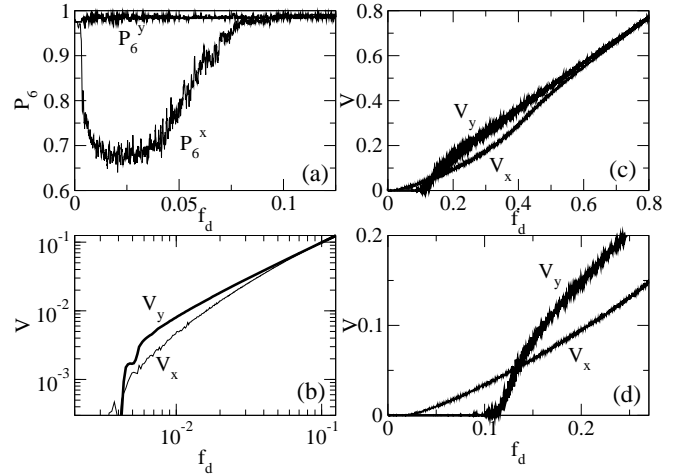


FIG. 4. (a) P_6 vs driving force f_d for a system with $f_p = 0.04$ at $T = 0$. Upper curve: P_6^y for $\mathbf{f}_d = f_d \hat{\mathbf{y}}$. Lower curve: P_6^x for $\mathbf{f}_d = f_d \hat{\mathbf{x}}$. (b) Average velocities vs f_d for the same system. Upper curve: V_y for $\mathbf{f}_d = f_d \hat{\mathbf{y}}$. Lower curve: V_x for $\mathbf{f}_d = f_d \hat{\mathbf{x}}$. (c) V_x and V_y vs f_d for a system with $f_p = 0.2$. (d) A blowup of (c) in the region near depinning showing the crossing of the velocity force curves.

translational order, so that for a wide range of temperatures and disorder strengths the system behaves as a 2D Bragg glass [14]. In the vortex liquid crystal case there are two length scales associated with the hard and soft directions, and the disorder induced dislocations first form in the soft direction. It may be possible that, on very large length scales, dislocations in the hard direction will also appear. For the parameters considered here, dislocations are present except at the lowest pinning strengths, roughly indicated by a dashed line in Fig. 3, where a 2D anisotropic Bragg glass forms.

We next consider dynamical effects in the presence of pinning. In the smectic-A state, there should be distinct transport signatures for the hard and soft directions. When the disorder is strong enough to destroy the smectic phase, there may still be an anisotropic transport signature if the system retains some form of nematic order. We first consider the pinned smectic-A state found at $f_p = 0.04$ and $T = 0$. We perform separate simulations for driving in the soft direction, $\mathbf{f}_d = f_d \hat{\mathbf{x}}$, and the hard direction, $\mathbf{f}_d = f_d \hat{\mathbf{y}}$, increasing the applied drive very slowly to avoid any transient effects. In Fig. 4(b) we plot $V_y = (1/N_v) \langle \sum_i^{N_v} v_y \rangle$ (upper curve) for driving in the hard direction and $V_x = (1/N_v) \langle \sum_i^{N_v} v_x \rangle$ (lower curve) for driving in the soft direction. Here, $V_x < V_y$, indicating that motion in the soft direction is easier except at very high drives when the effects of the pinning are washed out and the two curves come together. In Fig. 4(a) we plot P_6 for the two different driving directions. At $f_d = 0$, P_6 is slightly less than one due to the presence of a small number of dislocations in the smectic state. For depinning in the hard direction, P_6^y (upper curve), the system depins *elastically* without a prolifera-

tion of defects, and the vortices do not exchange neighbors as they move. For driving in the easy direction, P_6^x (lower curve) drops substantially when the vortices depin *plastically*, and a portion of the vortices remain pinned while others flow past. The effective pinning is known to be higher for a soft system where defects can proliferate than for an elastic system [15]. A similar proliferation of defects has been associated with the so called peak effect, where there is a sudden increase in the effective pinning force as a function of temperature or applied magnetic field [15]. At high drive, the system shifts from plastic flow to a dynamically reordered state [12] as indicated by the increase in P_6^x in Fig. 4(a), as well as by the merging of V_x and V_y in Fig. 4(b). These results imply that, in the pinned smectic-A state, the depinning is elastic in the hard direction and plastic in the soft direction. Further, the elastic and plastic depinning transitions produce different scaling responses in the velocity force curves. At depinning, the velocity scales with the driving force in the form $V = (f_d - f_c)^\beta$ [13]. For the plastic flow regime we find $\beta > 1.0$ while in the elastic flow regime we find $\beta < 1.0$, in agreement with theoretical expectations.

At finite temperatures and for f_p large enough that we observe only plastic depinning in both directions, we observe that the critical depinning force in the soft direction, f_c^x , is *lower* than the depinning force in the hard direction, f_c^y , even though $V_x < V_y$ at intermediate drives. This implies that the anisotropic flow exhibits a reversal from $V_x > V_y$ to $V_x < V_y$ at low drives. We explicitly demonstrate this effect for a system with $f_p = 0.25$ and $T = 0.25$ in Fig. 4(c,d). Here, the depinning is plastic in both directions, and the depinning forces are $f_c^x = 0.015$ and $f_c^y = 0.11$. There are fewer dislocations for $\mathbf{f}_d = f_d \hat{\mathbf{y}}$ and the system reorders at $f_d^y = 0.2$. For $\mathbf{f}_d = f_d \hat{\mathbf{x}}$, the system does not reorder until $f_d^x = 0.8$. There is a clear crossing of the velocity force curves at $f_d = 0.13$ so that the flow is easier in the soft direction for $f_d < 0.13$ and easier in the hard direction for $f_d > 0.13$. In Fig. 4(d) we show a blowup of this region. The crossing of the velocity force curves can be understood by considering that the depinning in the soft direction is plastic. At low drives, individual vortices can be thermally activated, giving rise to creep. For driving in the hard direction, the depinning is elastic and individual vortex hopping is not possible, so that only collective creep can occur. In the case of the nematic phase, when there is some plastic flow in the y -direction, there is still a large correlated length scale that must move so thermal effects are greatly reduced. Thus, creep in the pinned smectic phase and pinned nematic phase is enhanced in the soft direction compared to the hard direction. Even for very high values of f_p we observe an intermediate anisotropic response, suggesting the system can be considered a pinned nematic phase.

In conclusion, we have performed simulations of the recently proposed vortex liquid crystal state where the vortex-vortex interactions are anisotropic. We find that,

in the absence of disorder, the system shows an intermediate melting into a smectic-A state as proposed theoretically in Ref. [1]. The smectic-A state contains a small fraction of dislocations which are all aligned in the soft direction. In the presence of disorder, a pinned smectic-A state can occur, and the system depins plastically in the soft direction but elastically in the hard direction. We predict that, for equal intermediate drives, the velocity in the soft direction will be lower than in the hard direction. At finite temperatures the creep is much higher in the soft direction due to the fact that individual vortex hopping can occur, whereas creep is suppressed in the hard direction since the vortex motion is much more correlated. For high temperatures and disorder strengths, the system is disordered. For strong disorder the anisotropic transport should still be observable in the pinned nematic phase. We note that many of our results may apply to electron liquid crystals as well.

We thank E. Carlson for useful discussions. This work was supported by the U.S. Department of Energy under Contract No. W-7405-ENG-36.

-
- [1] E.W. Carlson, A.H. Castro Neto, and D.K. Campbell, Phys. Rev. Lett. **90**, 087001 (2003).
 - [2] X. Hu and Q.H. Chen, Phys. Rev. Lett. **92**, 209701 (2004).
 - [3] E.W. Carlson, A.H. Castro Neto, and D.K. Campbell, Phys. Rev. Lett. **92**, 209702 (2004).
 - [4] C. Eisenmann, U. Gasser, P. Keim, and G. Maret, Phys. Rev. Lett. **93**, 105702 (2004).
 - [5] E. Fradkin and S.A. Kivelson, Phys. Rev. B **59**, 8065 (1999).
 - [6] L. Radzihovsky and A.T. Dorsey, Phys. Rev. Lett. **88**, 216802 (2002).
 - [7] M.P. Lilly *et al.*, Phys. Rev. Lett. **83**, 824 (1999).
 - [8] K.B. Cooper *et al.*, Phys. Rev. B **65**, 241313 (2002).
 - [9] L. Balents and D.R. Nelson, Phys. Rev. B **52**, 12951 (1995).
 - [10] Q.-H. Wei, C. Bechinger, D. Rudhardt, and P. Leiderer, Phys. Rev. Lett. **81**, 2606 (1998); L. Radzihovsky, E. Frey, and D.R. Nelson, Phys. Rev. E **63**, 031503 (2001); J. Baumgartl, M. Brunner, and C. Bechinger, Phys. Rev. Lett. **93**, 168301 (2004).
 - [11] L. Balents, M.C. Marchetti and L. Radzihovsky, Phys. Rev. B **57**, 7705 (1998).
 - [12] K. Moon, R.T. Scalettar and G.T. Zimányi, Phys. Rev. Lett. **77**, 2778 (1998); C.J. Olson, C. Reichhardt, and F. Nori, Phys. Rev. Lett. **81**, 3757 (1998).
 - [13] D.S. Fisher, Phys. Rev. B **31**, 1396 (1985).
 - [14] P. Le Doussal and T. Giamarchi, Physica C **331**, 233 (2000).
 - [15] M.J. Higgins and S. Bhattacharya, Physica C **257**, 232 (1996).